Synthesis of Core-Shell Fluoroacrylate Copolymer Latex via Emulsion Polymerization and Its Application in Ink-Jet Ink

Xuefeng Li,[1,2] Jingfang Zhang,[1,2] Xingping Zhou,[3] Chuan Lu,[1] Xiantao Tong,[1] Guoxing He,[4] Xiaqin Wang[1,2]

[1]*College of Material Science and Engineering, Donghua University, Shanghai 201620, People's Republic of China*
[2]*State Key Laboratory for Modification of Chemical Fibers and Polymer Materials, Donghua University, Shanghai 201620, People's Republic of China*
[3]*College of Chemical Engineering and Biotechnology, Donghua University, Shanghai 201620, People's Republic of China*
[4]*College of Science, Donghua University, Shanghai 201620, People's Republic of China*

Received 15 September 2011; accepted 15 December 2011
DOI 10.1002/app.36679
Published online in Wiley Online Library (wileyonlinelibrary.com).

ABSTRACT: Core-shell fluoroacrylate copolymer latex was synthesized via semicontinuous seed emulsion polymerization, in which ethyl acrylate was utilized to prepare core, and methyl methacrylate, butyl acrylate, methacrylate acid, and hexafluorobutyl methacrylate were employed to constitute the shell. So the yielded latex particles had the soft core and hard shell. Multifunction and low viscosity of the latex had been applied as the binder of latex inks. The ζ potential showed that the latex particles had high thermodynamic stability. The latex and latex inks exhibited viscosity plateau of Newtonian fluid behaviors. Rheological tests revealed that viscous behaviors dominated in the latex and latex inks. However, there was some interaction among the latex and pigment particles. The hydrophobicity of the cast films of the latex increased with the amount of the fluoroacrylate monomer. Fluorine tended to migrate to the interface between the cast film and air. Therefore, the hydrophobicity was derived from the fluorine enrichment phenomena on the top side of the cast films. © 2012 Wiley Periodicals, Inc. J Appl Polym Sci 000: 000–000, 2012

Key words: fluoroacrylate copolymer; core-shell structure; emulsion polymerization; rheological property

INTRODUCTION

Latex particles from emulsion polymerization bring advantages due to environmental, health care concerns, and easy application procedures as well. Latex has unique chemical and physical properties and various industrial applications, such as coating materials for textiles, buildings, leather, etc.[1,2] The core-shell latex includes two or more layers compared with common monolayer latex. Different layers in core-shell latex provide different performance and enlarge their application fields.[3] Ink-jet printing is an innovative technique of recording images or patterns on various media surfaces for sign graphics. However, solvent-based ink-jet inks are still not environment friendly enough. Images are prone to fade because ink-jet inks have poor durability when exposed to sun and high humidity. Great improvement in printing area has been achieved in that latex acts as the binder of aqueous ink-jet inks, in which latex particles are dispersed homogenously in liquid vehicle of ink-jet inks, and latex particles deposited on substrate surface during ink-jet printing. Then a hydrophobic film could be formed on the substrate surface when the heating temperature reaches minimum film forming temperature (MFFT) of latex. The film entraps and protects colorants in latex inks.[4] Actually, the water resistance and mechanical properties of the film from latex are higher than the polymeric film from solvent-based inks. In particular, flow viscosity of latex is so low that latex is a kind of new potential binders for aqueous ink-jet inks.

Fluorine-containing polymers played important roles in the fields such as surface coatings, optical communication, and microelectronics due to their thermal stability, chemical resistance, hydrophobicity/oleophobicity, low surface energy/refractive index, and low dielectric constant.[5,6] Emulsion polymerization is one of the most important methods to prepare fluoropolymer. Fluoroacrylate emulsion has attracted much interest for their excellent surface properties. There are mainly two methodologies to prepare fluoroacrylate latex: (1) to copolymerize fluorine-containing acrylate with acrylate monomers;

Correspondence to: X. Wang (xqwang@dhu.edu.cn) or X. Zhou (xpzhou@dhu.edu.cn).

(2) to introduce fluorine-containing structure via reaction characteristics of epoxy groups.[7] However, high prices of fluorinated acrylate monomers limited their use. Core-shell latex has typical advantages compared with common monolayer latex.[8] So far as particles composed of fluorine-free core and fluorine-containing shell are concerned, core layer provides adhesion on substrates, and fluorine in shell migrates to the top surfaces during film formation process.[9,10] Therefore, the anticipated hydrophobicity of film could be obtained via core-shell latex while the amount of fluorinated monomers could be minimized.

The rheological properties and stability of latex are of great significance for exploiting the performance of novel aqueous ink-jet printing inks. Latex inks are similar with coating paints, although there are evident differences in flow behaviors. The latex inks are usually stored for a long period before their use. Latex particles normally tend to flocculate due to interaction among particles. Therefore, excellent dispersion stability of latex is expected to avoid flocculation. The rheological behaviors of latex are essential to avoid deflections in printer heads. Among the rheological properties, latex viscosity is the most important parameter of latex ink. Latex ink should have constant and low viscosity (4–10 mPa s) under high shear rates of nozzles.[11] However, most of latex generally exhibits non-Newtonian behaviors under shearing forces.[12] The factors affecting the latex viscosity involve polymer type, concentration, particle size, emulsifier content, temperature, and shear rate, and so on.[1]

Core-shell fluoroacrylate copolymer latex was prepared and characterized in this research. High stability, low viscosity, core-shell nanostructure, and good hydrophobicity were desired to find alternative aqueous ink-jet inks to solvent or UV-curable inks. High stability ensured that latex can be stored for a long period without flocculation. Different characteristics of the core and shell enlarged the application range of latex inks in ink-jet printing. The flow properties of latex inks were the most important factors for ink-jet printing. The hydrophobicity of latex films increased the durability of ink-jet printed images in humid atmosphere. Latex could provide protection and strong adhesion when it was used as the binder of ink-jet printing inks.

EXPERIMENTAL

Materials

Ethyl acrylate (EA), butyl acrylate (BA), methyl methacrylate (MMA), and methacrylate acid (MAA) monomers were supplied by Sinopharm Chemical Reagent Co. Ltd., China. Solubility of EA, BA, and MMA is 1.5 g, 0.2 g, and 1.6 g in 100 g of water, respectively. Hexafluorobutyl methacrylate (HFBM) ($CH_2{=}C(CH_3){-}COO{-}CH_2{-}CF_2{-}CFH{-}CF_3$) was purchased from Aldrich (St. Louis, MO). The mixture of emulsifiers was composed of sodium lauryl sulfate (SDS) as anionic emulsifier, Surfynol 465 (465) as nonionic surfactant (supplied by Sangjing Chemical Co. Ltd., Shanghai) with the mass ratio of 1 : 1. Potassium persulfate (KPS) was used as initiator and sodium bicarbonate ($NaHCO_3$) as buffering reagent.

Synthesis of core-shell fluoroacrylate latex

The core-shell fluoroacrylate latex was prepared via semicontinuous seed emulsion polymerization with two steps because the reaction rate of semicontinuous seed emulsion polymerization with two steps was much milder than that of simple one step batch process. All the polymerization steps were carried out under the protection of nitrogen atmosphere in a 250-mL four-neck flask equipped with a reflux condenser, and a mechanical stirrer (the mixing speed was 260–300 rmp).

Initially, EA (15.0 g) was emulsified by the mixed emulsifier (0.9 g, the mass ratio of SDS : 465 = 1 : 1) in deionized water (20.0 g) at 30°C for 0.5 h. The anionic surfactant SDS provided repulsive force between two similarly charged electric double layers of two neighboring latex particles. By contrast, the nonionic surfactant 465 imparted two neighboring latex particles with steric stabilization.[13] Then, 1/3 of the emulsified EA was added into the flask and heated to 80°C. The initiator KPS aqueous solution (5.0 g, 0.6 wt %) was added subsequently when the reaction temperature was 80°C, and this temperature was kept for 0.5 h. Simultaneously, the residual emulsified EA and KPS aqueous solution (10.0 g, 0.6 wt%) were added into the flask for 3 h for the synthesis of the core. Secondly, the admixture of the KPS aqueous solution (15.0 g, 0.6 wt %) and mixed emulsifier (0.3 g, the mass ratio of SDS : 465 = 1 : 1), BA (5.0 g), MMA (9.1 g), MAA (0.9 g), and HFBM monomer were added to form shell layer during next 3 h. The amounts of HFBM monomer were 0 g, 0.3 g, 0.9 g, 1.5 g, 2.1 g, and 2.7 g for Runs 0–5, respectively. The reaction was carried out for another 0.5 h. Finally, the reaction temperature was lowered to 25°C, and the reaction was terminated by the addition of $NaHCO_3$ (pH = 6–7). The solid contents of the yielded core-shell latex were 39.1%, 39.7%, 39.3%, 40.5%, 40.1%, and 40.8% for Runs 0–5, respectively.

Characterization

The particle size and distribution of the synthesized emulsion was characterized by particle size and ζ potential analyzer (Malvern Instruments Company, UK). Fourier transform infrared (FTIR) spectrometric analyzer (Perkin–Elmer, Waltham, MA) was used to analyze the chemical structures of the latex films

TABLE I
Particle Size and Stability of Core-Shell Latex

Samples		Run 0	Run 1	Run 2	Run 3	Run 4	Run 5
Core	Particle size (nm)	61.3	65.1	60.6	57.4	57.3	63.2
	PDI	0.042	0.034	0.04	0.06	0.027	0.063
Final particles	Particle size (nm)	90.2	93.4	89.1	91.3	88.3	91.4
	PDI	0.039	0.04	0.024	0.059	0.032	0.038
	ζ potential (mV)	−35.4	−40.8	−42.7	−45.7	−48.8	−50.3
Long-term stability	Latex	0	0	0	0	0	0
	Latex ink	1	1	1	0	0	0

Long-term stability was tested by storing latex and latex ink in an oven at 70°C for 1 week. The ratings for long-term stability were from 0 to 5 with 0 being the best result, that is, no precipitation or flocculation occurred.

and surface chemical structures was analyzed by attenuated total reflection-fourier transform infrared spectroscopy (ATR-FTIR) in the range from 400 to 4000 cm^{-1} in transmission. Contact angles (CAs) were measured on the basis of the sessile drop method at room temperature using a JY-82 CA goniometer. The glass transition temperature (T_g) of the latex was measured by differential scanning calorimeter (DSC, Perkin–Elmer, USA). The viscosity, storage modulus (G'), and loss modulus (G'') of the latex were measured by Advanced Rheology Expanded Systems (ARES-RFS, rheometer). The viscosity of latex and latex inks was obtained in the range of shear rate $\dot{\gamma}$ from 0.1 to 10^3 s^{-1}. The modulus was tested under 200% strain amplitude and angular frequency was from 0.1 to 100 s^{-1}. The morphology of the latex particle was observed with transmission electron microscopy (TEM, H-800, Hitachi, Japan). The latex particles were stained with phosphotungstic acid (2 wt %, pH 6.4) before TEM observation.

RESULTS AND DISCUSSION

Particle size and stability of the latex

The particle sizes and stability of the latex were summarized in Table I. All the latex particle sizes and polydispersity index (PDI) from Runs 0–5 were less than 100 nm and 0.1, respectively. In addition, the absolute values of ζ potential were larger than 30 mV, which means that the latex particles had high stability in water. The stability was derived from electrostatic interaction and steric stabilization of the shells among the latex particles. The absolute values of ζ potential increased with the amount of the fluorinated acrylate monomer, indicating that the fluorinated monomer might contribute to the stability of the emulsion. The long-term stability of the latex and latex ink was sufficient, because the types and fractions of the monomers in the shells were selected to obtain the hydrophilic shells with theoretical T_g 34°C to afford high reservation stability in water under a wide range of temperatures.

The following discussion took the results of Run 5 as example because the results of each run were similar. The particle size distribution for Run 5 was showed in Figure 1. The average size of the seeds and final latex particles was 63.2 nm and 91.4 nm, respectively, and the particles sizes exhibited monomodal distribution. It could be revealed that the final latex was of core-shell nanostructure from the size difference between the core and final particles.

In TEM micrograph of Run 5 (Fig. 2), a significant contrast between core (light regions) and shell (dark regions) of the latex particles could be observed clearly, which evidently proved the formation of the core-shell structure. TEM micrograph revealed effectively the core-shell structure of the latex particles obtained by semicontinuous seed emulsion polymerization method. The average diameter of the spherical core-shell particles was 100 ± 25 nm, and the average thickness of the shell was about 20 nm.

Rheological properties of latex and latex ink

The flow behavior of the latex and latex ink varied with shear rate in Figure 3. The viscosity of the latex showed a shear-thinning behavior under low shear rate. The latex showed a viscosity plateau of a Newtonian fluid behavior subsequently when the shear rate was higher than 60 s^{-1}. The latex particles

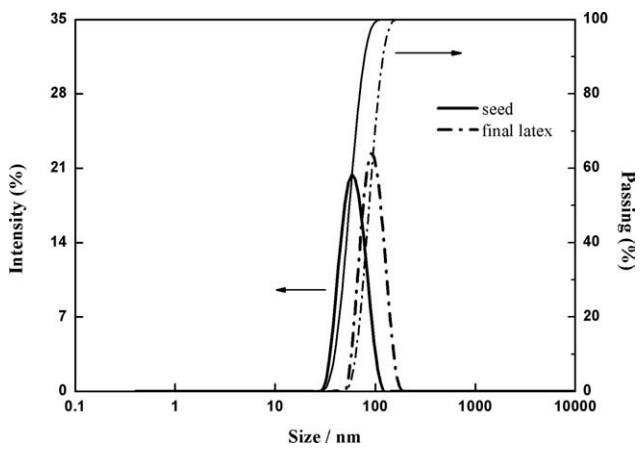

Figure 1 Particle sizes and distribution of core and final latex for Run 5.

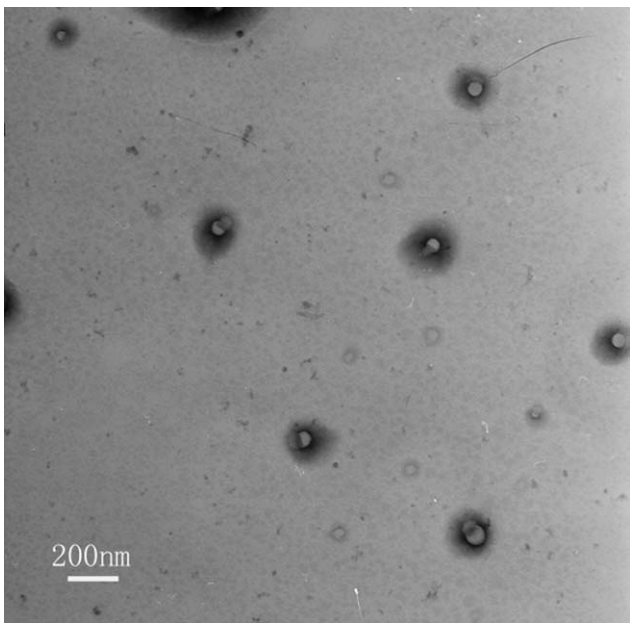

Figure 2 TEM image of latex particles from Run 5.

seemed to be independently dispersed in water, which was contrary to most polymers. Polymers have a tendency to entangle with their neighboring macromolecules chains, but the latex particles seemed to have no interaction with each other even under higher shear rates, because the types and fractions of the monomers in the shells were selected to obtain the hydrophilic shells with high T_g to afford high stability in water. The viscosity of the latex ink was lower than the corresponding latex under low shear rates, which might be caused by interaction between the latex and pigment particles. The viscosity of the latex ink was influenced by the size ratio and PDI of the latex particles and pigment particles.[14] However, the viscosity of the latex ink increased to the constant value even at low shear rates featuring

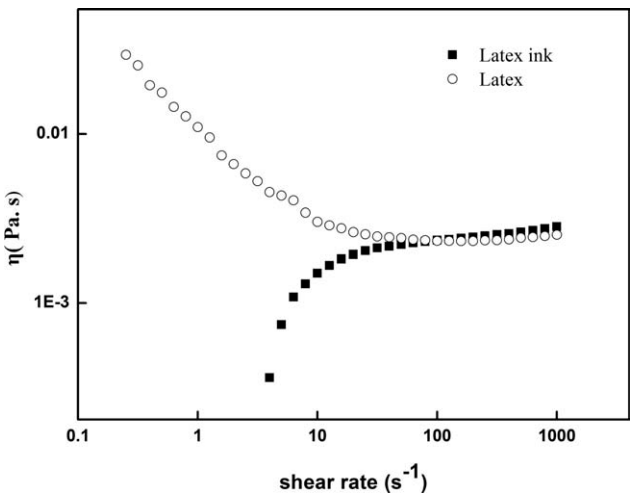

Figure 3 Steady shear viscosity η of 20 wt % latex from Run 5(○), and its latex ink (■).

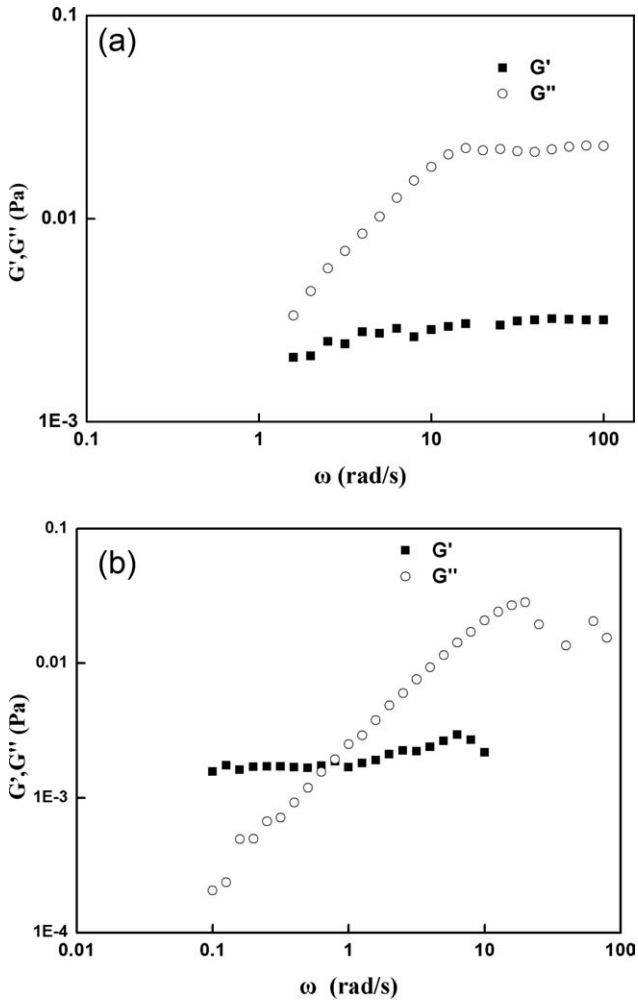

Figure 4 Dynamic shear modulus of latex for (a) the latex (20 wt %, Run 5) and (b) its latex ink. G' (■), G'' (○).

Newtonian fluid behavior. Finally, the viscosity of the latex ink was equal to that of the latex when the shear rate was above 100 s^{-1}.

Figure 4(a,b) depicts storage modulus (G') and loss modulus (G'') versus the angular frequency (ω) under a constant amplitude strain in the linear viscoelastic range of the samples. In Figure 4(a), G'' had higher values than G' in all frequency range, indicating that the viscous behavior dominated in the latex. G' was frequency independent corresponding to the plateau relaxation zone. There was no gel formation in the emulsion, which further accounted for the emulsion stability. G' and G'' were of the same order of magnitude for both the latex and latex ink, respectively, indicating that G' and G'' were influenced little by the latex and pigment particles. In Figure 4(b), there was intersection between the G' and G'' curves at low ω, which made it clear that interaction among the latex and pigment particles was inevitable in the latex ink. Perhaps some new structures composed of the latex and pigment particles occurred even at low ω of 1 s^{-1}.

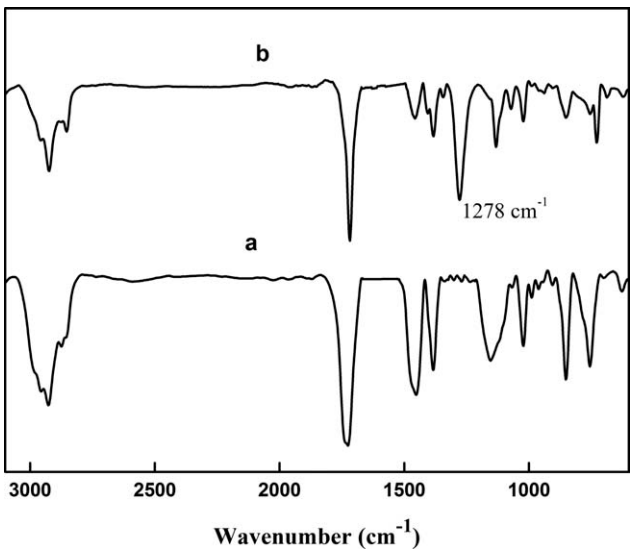

Figure 5 FTIR spectra of cast films of (a) the fluorine-free acrylate latex (Run 0) and (b) the fluorine-containing acrylate latex (Run 5).

Analyses of chemical structures of latex

Figure 5(a,b) shows the FTIR spectra of the cast films from the fluorine-free acrylate latex (Run 0) and fluorine-containing acrylate latex (Run 5), respectively. The absorption peak at 1640 cm^{-1} for C=C stretching vibration disappeared in both Figure 5(a,b), indicating that most of the monomers were involved in the copolymerization. Moreover, the stretching vibration of C—F bonds at 1278 cm^{-1} appeared in Figure 5(b), indicating that HFBM participated in the copolymerization.

Core-shell structures of latex

Figure 6 shows the DSC curves of the latex from Runs 0 and 5. T_g of Run 5 was observed at −16°C and 40°C [Fig. 6(a)], and T_g of Run 0 was −16°C and 38°C [Fig. 6(b)], respectively. So the HFBM content had no

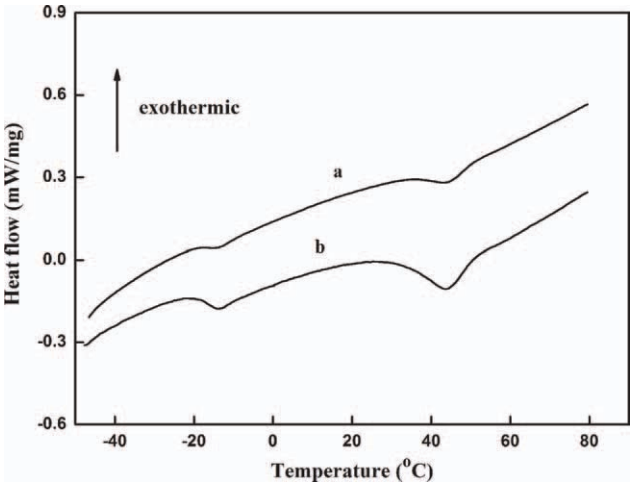

Figure 6 DSC curves of polyacrylate emulsion films from (a) Run 0 and (b) Run 5.

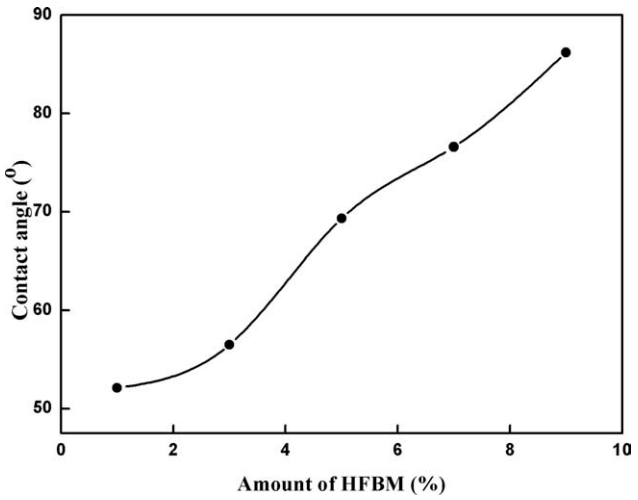

Figure 7 Influence of hydrophobicity of film surface on amount of HFBM.

significant impact on T_g of the shells. According to the feeding recipes, two theoretically calculated T_g should be −20°C for the core and 34°C for the shell based on the Fox equation. So the theoretical and measured T_g was in close agreement. The soft core of the core-shell structure provided strong adhesion on polymeric substrates, while the shell provided stability in aqueous phase and hydrophobicity for solid film.

Hydrophobicity of film surface

CA is a criterion for hydrophobicity of cast films from the latex. HFBM is of 46 wt % fluorine. Fluorinated side chains could migrate to the interface during film formation, which decreased the surface energy of the cast films substantially. The good hydrophobicity arose from the low surface energy. In Figure 7, the surface CA increased with the amount of HFBM, indicating that more fluorine had migrated to the film surface as shown in Figure 8. However, the fluorine-containing cast film had different hydrophobicity for the Side A and B as shown in Figure 9(a,b). It was obvious that most fluorine had migrated to the interface between the cast film and air (Side A in Fig. 8), and little could migrated to the other opposite Side B.[5,15]

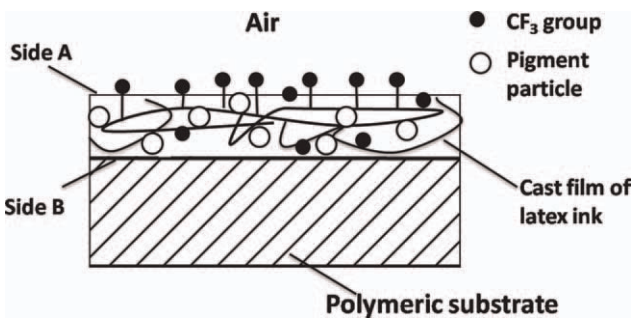

Figure 8 Schematic illustration for cast film of fluorine-containing latex.

Figure 10 provides the ATR-FTIR spectra of the cast film from Run 5, which could explain fluorine migration to some extent. The absorption peak at 1278 cm^{-1} was ascribed to the stretching vibration of C—F bonds in Figure 5(b). However, the absorption peak moved to 1241 cm^{-1} and 1174 cm^{-1} in Figure 10(a,b), corresponded to stretching vibration of C—F bonds. Moreover, the absorption of C—F bonds was much stronger in Figure 10(a) than in Figure 10(b) and Figure 5(b), which revealed that fluorine migrated and gathered on the interface between the cast film and air (Side A in Fig. 8).

CONCLUSIONS

The core-shell nanostructured fluoroacrylate latex particles were synthesized via semicontinuous seed emulsion polymerization. The soft core of the core-shell structures provided strong adhesion on polymeric substrates, while the shell provided stability in aqueous phase and hydrophobicity for solid film. The FTIR spectra confirmed that the fluorined acrylate monomer had been involved in the copolymerization. The ζ potential revealed that the emulsion stability was improved by introduction of the fluorinated monomer. The viscosity of the latex and latex inks exhibited Newtonian fluid behaviors. The MFFT was high enough to avoid clogging of nozzles, which was very important for ink-jet printing when the inks were jetted from nozzles. CAs revealed that surface hydrophobicity was enhanced by fluorine migration. These interesting phenomena may have valuable utility for the nanostructured latex as a new kind of resin binders in aqueous ink-jet printing inks. Latex inks will offer important benefits to commercial and industrial production environments. No hazardous volatile organic compounds are released into air creating an improved printing environment.

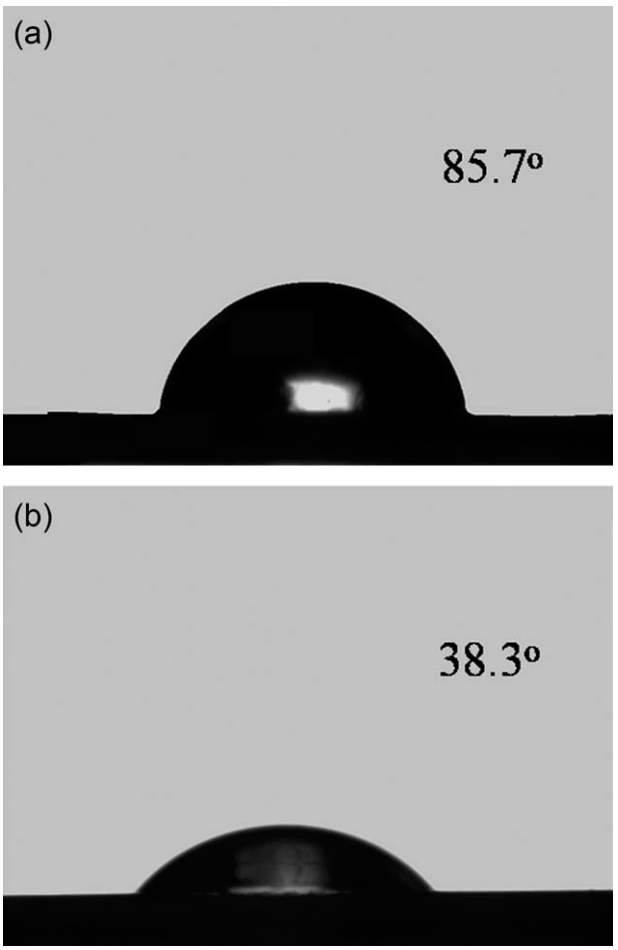

Figure 9 CAs of fluorine-containing cast film from Run 5 on (a) Side A, and (b) Side B.

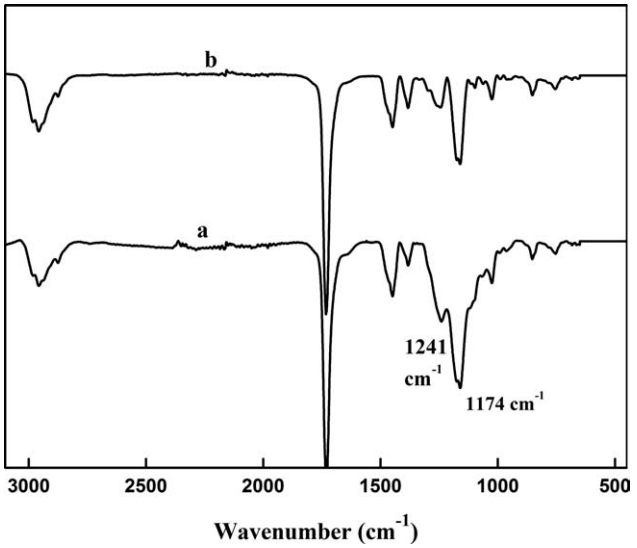

Figure 10 ATR-FTIR spectra of cast film from Run 5 on (a) Side A and (b) Side B.

References

1. Yılmaz, O.; Cheaburu, C. N.; Gülümser, G.; Vasile, C. Prog Org Coat 2011, 70, 52.
2. Chesne, A. D.; Bojkova, A.; Gapinski, A.; Seip, D.; Fischer, P. J Colloid Interface Sci 2000, 224, 91.
3. Tolue, S.; Moghbeli, M. R.; Ghafelebashi, S. M. Eur Polym J 2009, 45, 714.
4. Vincent, K. D.; Ganapathiappan, S. U.S. Pat. 7,371,273 B2 (2008).
5. Xiao, X. Y.; Wang, Y. Colloids Surf A 2009, 348, 151.
6. He, L.; Liang, J. Y. J Fluorine Chem 2008, 129, 590.
7. Chen, L. J.; Shi, H. X.; Wu, H. K. Colloids Surf A 2010, 368, 148.
8. Cheng, X. L.; Chen, Z. X.; Shi, T. S.; Wang, H. Y. Colloids Surf A 2007, 292, 119.
9. Xiao, X. Y.; Liu, J. F. Chin J Chem Eng 2008, 16, 626.
10. Liang, J. Y.; He, L.; Zheng, Y. S. J Appl Polym Sci 2009, 112, 1615.
11. Leelajariyakul, S.; Noguchi, H.; Kiatkamjornwong, S. Prog Org Coat 2008, 62, 145.
12. Molenaar, F.; Svanholm, T.; Toussaint, A. Prog Org Coat 1997, 30, 141.
13. Chern, C. S. Prog Polym Sci 2006, 31, 443.
14. Schneider, M.; Claverie, J.; Guyot, A. J Appl Polym Sci 2002, 84, 1878.
15. X. J. Cui, Zhong, S. L.; Wang, H. Y. Colloids Surf A 2007, 303, 173.